Tectonic controls on fault zone flow pathways in the Rio Grande rift, New Mexico, USA

Randolph T. Williams[1], Laurel B. Goodwin[1], Peter S. Mozley[2], Brian L. Beard[1], and Clark M. Johnson[1]
[1]Department of Geoscience, University of Wisconsin–Madison, Madison, Wisconsin 53706, USA
[2]Department of Earth and Environmental Science, New Mexico Institute of Mining and Technology, Socorro, New Mexico 87801, USA

ABSTRACT

We assessed tectonic controls on the spatial and temporal distribution of fault zone flow pathways in the Rio Grande rift (New Mexico, USA) by using fault zone calcite cements as a geochemical record of syntectonic fluid flow. Cement $\delta^{18}O$, $\delta^{13}C$, and $^{87}Sr/^{86}Sr$ values indicate that older, large-displacement master and basin-margin faults were cemented by more isotopically evolved basinal brines than younger intrabasin faults. These data suggest that diagenetic fluids in basin-bounding faults equilibrated predominantly with downdip Paleozoic carbonates. In contrast, intrabasin faults transmitted fluids from shallow stratigraphic sources. This pattern of flow pathways is linked to the systematic distribution of sediments and faults that record rift evolution, which dictated spatial and temporal variations in fault zone architecture and permeability structure. Our results indicate that the depths from which fluids can be transported in active rift basins ultimately depend on both tectonically mediated variations in the grain size of syntectonic sediments entrained in fault damage zones and fault displacement magnitude.

INTRODUCTION

Understanding basin-scale subsurface fluid flow is critical to petroleum exploration (e.g., Bethke et al., 1991; Gong et al., 2011), geological CO_2 sequestration (e.g., Birkholzer et al., 2009; Person et al., 2010), and contaminant transport modeling (e.g., Carle et al., 2006). In rift basins, factors affecting regional flow patterns include variations in sediment type (Person and Garven, 1994; Mailloux et al., 1999), basin subsidence and/or compaction (Cathles and Smith, 1983; Cartwright, 1994), and hydrothermal circulation (Person and Garven, 1992; Simms and Garven, 2004). Faults included in regional flow models are often treated as discrete boundaries with no intrinsic permeability (Mailloux et al., 1999). Few previous studies have explicitly considered fault zone fluid transport (cf. Simms and Garven, 2004; Guillou-Frottier et al., 2013), despite the fact that fault zones can be distinct hydrologic units with measurable permeability anisotropy (Rawling et al., 2001; Bense and Person, 2006), capable in some cases of transporting fluids from great depth to the surface (Crossey et al., 2006; Williams et al., 2013).

The systematic distribution of sediments and faults established during extension in rift basins (Gawthorpe and Leeder, 2000; Fig. 1A) suggests that fault zone permeability structure will vary with basin position, as the sediment or rock type cut by a fault exerts a primary control on fault zone architecture (Rawling et al., 2001). If correct, this hypothesis will help predict which faults serve as conduits for fluids from differing stratigraphic levels. We tested this hypothesis by field, microstructural, and geochemical studies of fault zone calcite cements (a geochemical record of fluid source) in different structural positions in the Rio Grande rift, New Mexico (USA) (Fig. 1B). We show that syntectonic fluid source depths varied systematically with fault zone structural position, providing, for the first time, an opportunity to examine the role of tectonic processes in determining the spatial and temporal distribution of fault zone flow pathways during basin development.

GEOLOGIC SETTING

Basins of the Rio Grande rift are bound by large normal faults (Fig. 1A; master and basin-margin faults) that accommodated the majority of extension since rifting began in the middle Oligocene (Chapin and Cather, 1994). In the Late Miocene, faulting near basin margins slowed, and subsidence was increasingly accommodated by numerous, relatively small displacement (<200 m) intrabasin faults that formed nearer basin axes. Middle Oligocene to Miocene basin fill (Fig. 1A; Lower Santa Fe Group, LSF) records closed-basin deposition, and grades from coarse-grained, high-permeability alluvial fan and fluvial deposits near uplifted basin margins to fine-grained, low-permeability lacustrine and playa deposits nearer basin centers (Cather et al., 1994; Hawley et al., 1995). Pliocene–Pleistocene basin fill (Upper Santa Fe Group, USF) records the establishment of throughgoing axial drainage, and grades from basin-margin alluvial fan to eolian and fluvial sediments nearer basin centers. Most faults in the Rio Grande rift exhibit low-permeability clay-rich cores flanked by damage zones (Minor and Hudson, 2006). Where faults cut poorly lithified Santa Fe Group sediments, damage zone structures record particulate flow (mixed zones of Rawling et al., 2001; Rawling and Goodwin, 2006). Where faults cut fully lithified pre-rift units, damage zones are dominated by fracture networks (cf. Caine et al., 1996).

This spatial distribution of sediments and normal faults allows us to define three end-member fault types (Fig. 1A): (1) master faults, the largest displacement, basin-bounding faults, which juxtapose coarse-grained, high-permeability alluvial fans and lithified pre-rift units; (2) basin-margin faults, which have relatively large downdip displacements but juxtapose relatively coarse grained USF and LSF sediments near the surface; and (3) relatively small displacement, intrabasin faults that juxtapose fine-grained, low-permeability lacustrine and playa deposits of the LSF throughout much of their downdip extent. High-permeability hanging-wall damage zones of sheared, rift-margin sediments and footwall damage zones with a significant extent of fractured pre-rift units suggest that master and basin-margin faults may act as conduits for deep basinal brines (Fig. 1A). Conversely, damage zones of sheared, low-permeability LSF lacustrine and playa deposits should block flow between basement and USF damage zones, implying that intrabasin faults transport fluids between shallow fluvial and eolian aquifers of the USF. Calcite cement is common in these faults and oriented concretions locally record fault-parallel flow (Mozley and Goodwin, 1995; Minor and Hudson, 2006). Locally, cements are cut by fractures and slickenlines are evident between cemented damage zone and core, recording syntectonic cementation (Heynekamp et al., 1999). Determining the sources of fluids that precipitated these syntectonic fault cements is key to testing our hypothesis.

METHODS

We studied five representative fault types in the Albuquerque Basin (northern Albuquerque and Santo Domingo subbasins) and Socorro Basin (Fig. 1B). All have USF sediments in cemented hanging-wall damage zones, indicating that fluids were transported to similar stratigraphic levels. Fault names and locations, footwall characteristics, and additional details of hanging-wall sediments follow. (1) The La Bajada fault, a master fault of the Santo Domingo subbasin, has a footwall of Mesozoic sedimentary rocks. (2) The Loma Blanca fault, a Socorro basin-margin fault, juxtaposes Pleistocene alluvium and Pliocene fluvial sands. (3) An intrabasin transfer fault, here referred to as the Santa Ana transfer, juxtaposes USF fluvial and eolian sands. (4) The informally named Arroyo Sediento intrabasin fault juxtaposes USF fluvial sands. (5) The Sand Hill basin-

GEOLOGY, August 2015; v. 43; no. 8; p. 723–726 | Data Repository item 2015248 | doi:10.1130/G36799.1 | Published online 1 July 2015

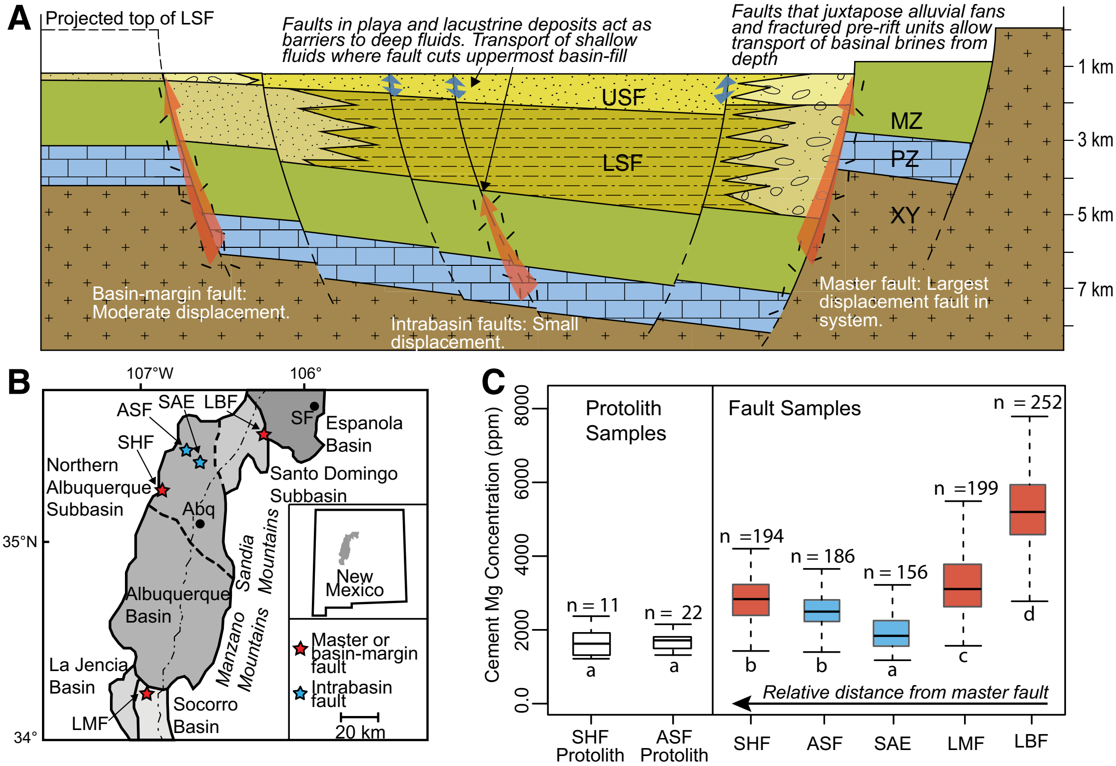

Figure 1. A: Simplified schematic cross section of the Albuquerque Basin (southwestern USA) showing basin asymmetry, end-member fault types, and hypothesized flow pathways. Lithologic units: USF—Upper Santa Fe Group (Pliocene–Pleistocene); LSF—Lower Santa Fe Group (middle Oligocene–Miocene); MZ—Mesozoic sedimentary units; PZ—Paleozoic carbonate units; XY—Proterozoic crystalline basement. Full lithologic variability of LSF and USF sediments is not shown. B: Study sites within selected basins of the Rio Grande rift, New Mexico. Red stars show master or basin-margin faults: LBF—La Bajada; SHF—Sand Hill; LMF—Loma Blanca. Blue stars show intrabasin faults: SAE—Santa Ana transfer; ASF—Arroyo Sediento. Black dots are cities: Albuquerque (Abq) and Santa Fe (SF). Adapted from Mozley and Goodwin (1995). C: Box plots of fault cement Mg concentration as a function of relative distance from the basin master fault; protolith cement concentrations shown for comparison. Letters a–d show statistically significant groups at the 95% confidence level; n = number of electron microprobe measurements; tails at 5th and 95th percentiles.

margin fault has a footwall of LSF sediments. The latter three faults are located in the northern Albuquerque subbasin.

The distribution and character of fault zone structures, lithologic units, and mesoscale cement paragenesis were documented at each site. Samples were collected from well-cemented portions of fault zones, which in these faults are restricted to hanging-wall damage zones. Modal mineralogy was determined by point counting. We selected a subset of samples from each fault for electron microprobe, oxygen, carbon, and strontium isotope analyses. Details of methods and tabulated data are given in the GSA Data Repository[1].

RESULTS

Cements were precipitated in immature sands (Table DR1 in the Data Repository). Pore-filling calcite cement accounts for 20–60 vol% of the rocks. Sections cut perpendicular to fault strike display a well-defined shape-preferred orientation of elongate grains subparallel to each fault (Fig. DR1). In contrast, elongate grains outside of the fault zone are aligned parallel to bedding (Rawling and Goodwin, 2006). No evidence of multiple generations of calcite cement was found in either petrographic or backscattered electron images of samples. Cements are nonluminescent, and record no evidence of post-cementation deformation.

Fault cements are nearly pure calcite; Mg and Sr are the only trace elements detected by electron microprobe. Master fault cements are enriched in Mg and Sr relative to basin-margin and intrabasin fault cements (Figs. 1C and 2E). Intrabasin faults have the lowest Mg and Sr concentrations. Concentrations of Mg and Sr decrease systematically with distance from the master fault, then increase near basin-margin faults on the opposite side of a basin.

Fault calcite cement $^{87}Sr/^{86}Sr$, $\delta^{18}O$, and $\delta^{13}C$ values also show systematic trends as a function of fault position (Fig. 2). Master and basin-margin faults show relatively high $^{87}Sr/^{86}Sr$, $\delta^{18}O$, and $\delta^{13}C$ values compared to intrabasin faults. Master and basin-margin faults also show a relatively narrow range in $^{87}Sr/^{86}Sr$, $\delta^{18}O$, and $\delta^{13}C$ values, whereas intrabasin faults have nearly constant $\delta^{18}O$ and a wide range of $^{87}Sr/^{86}Sr$ and $\delta^{13}C$ values (Figs. 2A–2C).

DISCUSSION

Fault cement chemistry varies spatially in the Rio Grande rift (Figs. 1C and 2). We consider these variations in terms of fluid source to test our hypothesis that fault zone permeability structure varies systematically with basin position.

Precipitation from meteoric fluids is suggested by the comparatively low $\delta^{18}O$, low $\delta^{13}C$ (organic carbon), and Mg and Sr concentrations of intrabasin fault cements (Figs. 2A and 2E; cf. Plummer et al., 2004; Williams et al., 2013). Calcite precipitation temperatures of 4–22 °C calculated from cement $\delta^{18}O$ values assuming equilibrium fractionation (Kim and O'Neil, 1997) and modern meteoric water values for the study area (–10‰ to –14‰ Vienna standard mean ocean water, VSMOW; Kendall and Coplen, 2001) support this interpretation. Relatively low $^{87}Sr/^{86}Sr$ ratios of intrabasin fault cements can also be explained by precipitation from a fluid comparable in $^{87}Sr/^{86}Sr$ ratio to the Rio Grande river (headwater values of ~0.7096; Hogan et al., 2007), possibly following minor interaction with relatively young rift volcanic rocks (~0.7020–0.7080; McMillan, 1998).

Cementation by deep basinal brines is consistent with the higher $^{87}Sr/^{86}Sr$, $\delta^{18}O$, and $\delta^{13}C$ values in master and basin-margin fault cements. As meteoric fluids contain negligible Sr^{2+} concentrations and the Rio Grande headwaters have $^{87}Sr/^{86}Sr$ ratios of ~0.7096, cement $^{87}Sr/^{86}Sr$ > ~0.7100 in master and basin-margin faults indicate fluid input from deeper

[1]GSA Data Repository item 2015248, tabulated geochemical data, supplementary data plots, and detailed geochemical methodology, is available online at www.geosociety.org/pubs/ft2015.htm, or on request from editing@geosociety.org or Documents Secretary, GSA, P.O. Box 9140, Boulder, CO 80301, USA.

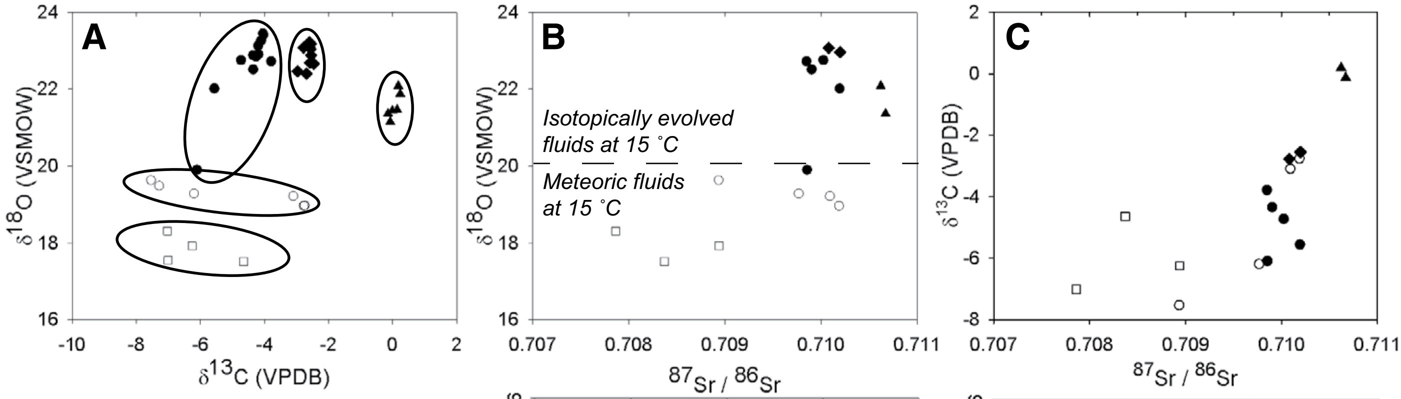

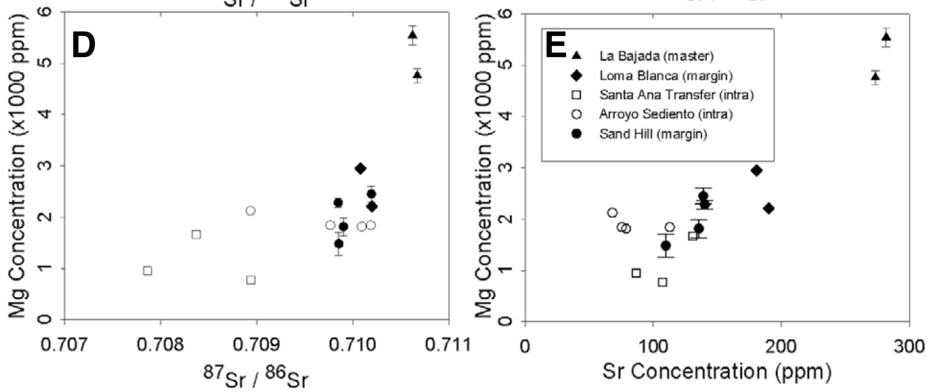

Figure 2. A: δ^{13}C and δ^{18}O of fault zone calcite cements. VSMOW—Vienna standard mean ocean water; VPDB—Vienna Peedee belemnite. B: δ^{18}O versus ^{87}Sr/^{86}Sr. C: δ^{13}C versus ^{87}Sr/^{86}Sr. D: Mg concentration versus ^{87}Sr/^{86}Sr. E: Mg concentration versus Sr concentration. Uncertainty is less than or equal to the size of plotted points where error bars are not shown. Filled symbols are master or basin-margin faults, open symbols are intrabasin faults. Dashed line is the divide between meteoric and isotopically evolved fluid values based on cement δ^{18}O and assumed 15 °C precipitation temperature. Tabulated data are available in Tables DR2–DR4 (see footnote 1).

(i.e., older) crustal sources (Banner, 1995; Crossey et al., 2006; Hogan et al., 2007; Williams et al., 2013). Carbon isotope data for these faults are also consistent with cementation by high δ^{13}C, deep basinal fluids (Fig. 2A), an interpretation supported by high concentrations of Mg and Sr (Figs. 1C and 2E). Furthermore, precipitation temperatures calculated for master and basin-margin fault cements using meteoric δ^{18}O values are improbably low (−8 to 9 °C), indicating an isotopically evolved fluid source. Deeply derived fluids associated with modern hot springs in the Rio Grande rift have δ^{18}O between −2‰ and 6‰ VSMOW (Williams et al., 2013), although some of these values may reflect evaporative enrichment.

The correlation between Mg and Sr in master and basin-margin fault cements and their ^{87}Sr/^{86}Sr, δ^{18}O, and δ^{13}C values are consistent with cementation by a fluid that equilibrated mainly with Paleozoic carbonate units (Fig. 1A). Williams et al. (2013) showed that dissolved inorganic carbon in Rio Grande rift waters was sourced in part from these units. This interpretation explains the positive correlation between cement ^{87}Sr/^{86}Sr, Mg and Sr concentration, and δ^{13}C, as marine limestones can provide substantial Mg^{2+}, Sr^{2+}, and near-zero δ^{13}C values to solution. Paleozoic carbonates are likely to have ^{87}Sr/^{86}Sr ratios of 0.7070–0.7084 (McArthur et al., 2001). Relatively radiogenic values documented here suggest minor fluid interaction with interbedded calcareous shales of the Madera Formation (>0.7100; Mukhopadhyay and Brookins, 1976; Williams et al., 2013) and/or underlying crystalline basement rocks (>0.7481; Taggart and Brookins, 1975). Observed trends in cement geochemistry likely record mixing between end-member meteoric and deep basinal fluids. We propose that the specific contributions of end-member fluids to the overall geochemical signal recorded in a given fault cement are ultimately tectonically controlled. Specifically, variations in grain size of the syntectonic sediments sheared in fault damage zones and fault displacement magnitude were the primary factors determining whether deep basinal fluids could be transported to the near surface (Fig. 1A).

CONCLUSIONS

Our data demonstrate that fault zone flow pathways varied systematically with structural position in the Rio Grande rift. In master and basin-margin faults, proximity to uplifted sediment sources resulted in hanging-wall damage zones of sheared, high-permeability alluvial fan and/or fluvial sediments; large displacements produced footwall damage zones with a significant extent of fractured pre-rift units. This fault zone architecture allowed transport of fluids from relatively deep stratigraphic levels to cement precipitation sites in high-permeability hanging walls. In contrast, intrabasin fault zones served as barriers to flow through LSF low-permeability lacustrine and playa deposits. However, they were conduits for meteoric fluids within high-permeability damage zones in the USF, where they likely shuttled water either upward or downward between adjacent aquifers (cf. Haneberg, 1995).

The temporal distribution of different fault permeability structures was also tectonically mediated during basin development. Master and basin-margin faults initiated with rifting; intrabasin faults formed later in rift history. We conclude that the extension history of the Rio Grande rift resulted in a predictable spatial and temporal distribution of fault zone flow pathways, which transmitted fluids from different stratigraphic levels depending on slip magnitude and basin position. All of the studied fault types extend from crystalline basement into USF basin-fill sediments (Russell and Snelson, 1994); therefore we conclude that downdip fault extent was not a primary control on fluid source depths. Our results provide a fundamental first step toward predicting regional flow patterns in extensional settings by improving our understanding of tectonic controls on the distribution of syntectonic fault zone flow pathways in sedimentary basins.

ACKNOWLEDGMENTS

S. Minor, D. Newell, and an anonymous reviewer provided constructive reviews. We thank the Santa Ana and Zia Pueblos for access to field sites. Work was supported by grants from the GDL Foundation, the Geological Society of America, the American Association of Petroleum Geologists, and the Wisconsin Alumni Research Foundation. We thank B. Link for field assistance, and S. Minor for outcrop locations.

REFERENCES CITED

Banner, J.L., 1995, Application of the trace element and isotope geochemistry of strontium to studies of carbonate diagenesis: Sedimentology, v. 42, p. 805–824, doi:10.1111/j.1365-3091.1995.tb00410.x.

Bense, V.F., and Person, M.A., 2006, Faults as conduit barrier systems to fluid flow in siliciclastic sedimentary aquifers: Water Resources Research, v. 42, W05421, doi:10.1029/2005WR004480.

Bethke, C.M., Reed, J.D., and Oltz, D.F., 1991, Long-range petroleum migration in the Illinois Basin (1): American Association of Petroleum Geologists Bulletin, v. 75, p. 925–945.

Birkholzer, J.T., Zhoi, Q., and Tsang, C.F., 2009, Large-scale impact of CO_2 storage in deep saline aquifers: A sensitivity study on pressure response in stratified systems: International Journal of Greenhouse Gas Control, v. 3, p. 181–194, doi:10.1016/j.ijggc.2008.08.002.

Caine, J.S., Evans, J.P., and Forster, C.B., 1996, Fault zone architecture and permeability structure: Geology, v. 24, p. 1025–1028, doi:10.1130/0091-7613(1996)024<1025:FZAAPS>2.3.CO;2.

Carle, S.F., Esser, B.K., and Moran, J.E., 2006, High-resolution simulation of basin-scale nitrate transport considering aquifer system heterogeneity: Geosphere, v. 2, p. 195, doi:10.1130/GES00032.1.

Cartwright, J.A., 1994, Episodic basin-wide fluid expulsion from geopressured shale sequences in the North Sea basin: Geology, v. 22, p. 447–450, doi:10.1130/0091-7613(1994)022<0447:EBWFEF>2.3.CO;2.

Cather, S.M., Chamberlin, R.M., Chapin, C.E., and McIntosh, W.C., 1994, Stratigraphic consequences of episodic extension in the Lemitar Mountains, central Rio Grande rift, *in* Keller, G.R., and Cather, S.M., eds., Basins of the Rio Grande Rift: Structure, Stratigraphy, and Tectonic Setting: Geological Society of America Special Paper 291, p. 157–170, doi:10.1130/SPE291-p157.

Cathles, L.M., and Smith, A.T., 1983, Thermal constraints on the formation of Mississippi Valley-type deposits and their implications for episodic basin dewatering and deposit genesis: Economic Geology and the Bulletin of the Society of Economic Geologists, v. 78, p. 983–1002, doi:10.2113/gsecongeo.78.5.983.

Chapin, C.E., and Cather, S.M., 1994, Tectonic setting of the axial basins of the northern and central Rio Grande rift, *in* Keller, G.R., and Cather, S.M., eds., Basins of the Rio Grande Rift: Structure, Stratigraphy, and Tectonic Setting: Geological Society of America Special Paper 291, p. 5–26, doi:10.1130/SPE291-p5.

Crossey, L.J., Fischer, T.P., Patchett, P.J., Karlstrom, K.E., Hilton, D.R., Newell, D.L., Huntoon, P., Reynolds, A.C., and de Leeuw, G.A.M., 2006, Dissected hydrologic system at the Grand Canyon: Interaction between deeply derived fluids and plateau aquifer waters in modern springs and travertine: Geology, v. 34, p. 25–28, doi:10.1130/G22057.1.

Gawthorpe, R.L., and Leeder, M.R., 2000, Tectono-sedimentary evolution of active extensional basins: Basin Research, v. 12, p. 195–218, doi:10.1046/j.1365-2117.2000.00121.x.

Gong, Z.S., Huang, L.F., and Chen, P.H., 2011, Neotectonic controls on petroleum accumulations, offshore China: Journal of Petroleum Geology, v. 34, p. 5–27, doi:10.1111/j.1747-5457.2011.00490.x.

Guillou-Frottier, L., Carrė, C., Bourgine, B., Bouchot, V., and Genter, A., 2013, Structure of hydrothermal convection in the Upper Rhine Graben as inferred from corrected temperature data and basin-scale numerical models: Journal of Volcanology and Geothermal Research, v. 256, p. 29–49, doi:10.1016/j.jvolgeores.2013.02.008.

Haneberg, W.C., 1995, Steady state groundwater flow across idealized faults: Water Resources Journal, v. 31, p. 1815–1820, doi:10.1029/95WR01178.

Hawley, J.W., Haase, C.S., and Lozinsky, R.P.I., 1995, An underground view of the Albuquerque Basin, *in* Ortega-Klett, C.T., ed., The Water Future of Albuquerque and the Middle Rio Grande Basin: Las Cruces, New Mexico Water Resources Research Institute, p. 37–55.

Heynekamp, M.R., Goodwin, L.B., Mozley, P.S., and Haneberg, W.C., 1999, Controls on fault zone architecture in poorly lithified sediments, Rio Grande rift, New Mexico: Implications for fault zone permeability and fluid flow, *in* Haneberg, W.C., et al., eds., Faults and subsurface fluid flow in the shallow crust: American Geophysical Union Geophysical Monograph 113, p. 27–49, doi:10.1029/GM113p0027.

Hogan, J.F., Phillips, F.M., Mills, S.K., Hendricks, J.M.H., Ruiz, J., Chesley, J.T., and Asmerom, Y., 2007, Geologic origins of salinization in a semi-arid river: The role of sedimentary basin brines: Geology, v. 35, p. 1063–1066, doi:10.1130/G23976A.1.

Kendall, C., and Coplen, T.B., 2001, Distribution of oxygen-18 and deuterium in river waters across the United States: Hydrological Processes, v. 15, p. 1363–1393, doi:10.1002/hyp.217.

Kim, S.T., and O'Neil, J.R., 1997, Equilibrium and nonequilibrium oxygen isotope effects in synthetic carbonates: Geochimica et Cosmochimica Acta, v. 61, p. 3461–3475, doi:10.1016/S0016-7037(97)00169-5.

Mailloux, B.J., Person, M., Kelley, S., Dunbar, N., Cather, S., Strayer, L., and Hudleston, P., 1999, Tectonic controls on the hydrogeology of the Rio Grande Rift, New Mexico: Water Resources Research, v. 35, p. 2641–2659, doi:10.1029/1999WR900110.

McArthur, J.M., Howarth, R.J., and Bailey, T.R., 2001, Strontium isotope stratigraphy: LOWESS Version 3: Best fit to the marine Sr isotope curve for 0–509 Ma and accompanying look-up table for deriving numerical age: Journal of Geology, v. 109, p. 155–170, doi:10.1086/319243.

McMillan, N.J., 1998, Temporal and spatial magmatic evolution of the Rio Grande rift, *in* Mack, G.H., et al., eds., Las Cruces Country II: New Mexico Geological Society Guidebook 49, p. 107–116.

Minor, A.S., and Hudson, M.R., 2006, Regional survey of structural properties and cementation patterns of fault zones in the northern part of the Albuquerque basin, New Mexico—Implications for ground-water flow: U.S. Geological Survey Professional Paper 1719, 28 p.

Mozley, P.S., and Goodwin, L.B., 1995, Patterns of cementation along a Cenozoic normal fault: A record of paleoflow orientations: Geology, v. 23, p. 539–542, doi:10.1130/0091-7613(1995)023<0539:POCAAC>2.3.CO;2.

Mukhopadhyay, B., and Brookins, D., 1976, Strontium isotopic composition of the Madera Formation (Pennsylvanian) near Albuquerque, New Mexico: Geochimica et Cosmochimica Acta, v. 40, p. 611–616, doi:10.1016/0016-7037(76)90107-1.

Person, M., and Garven, G., 1992, Hydrologic constraints on petroleum generation within continental rift basins: Theory and application to the Rhine graben: American Association of Petroleum Geologists Bulletin, v. 76, p. 468–488.

Person, M., and Garven, G., 1994, A sensitivity study of the driving forces on fluid flow during continental-rift basin evolution: Geological Society of America Bulletin, v. 106, p. 461–475, doi:10.1130/0016-7606(1994)106<0461:ASSOTD>2.3.CO;2.

Person, M., Banerjee, A., Rupp, J., Medina, C., Lichtner, P., Gable, C., Pawar, R., Celia, M., McIntosh, J., and Bense, V., 2010, Assessment of basin-scale hydrologic impacts of CO_2 sequestration, Illinois basin: International Journal of Greenhouse Gas Control, v. 4, p. 840–854, doi:10.1016/j.ijggc.2010.04.004.

Plummer, L.N., Bexfield, L.M., Anderholm, S.K., Sanford, W.E., and Busenburg, E., 2004, Hydrochemical tracers in the middle Rio Grande Basin, USA: 1. Conceptualization of groundwater flow: Hydrogeology Journal, v. 12, p. 359–388, doi:10.1007/s10040-004-0324-6.

Rawling, G.C., and Goodwin, L.B., 2006, Structural record of the mechanical evolution of mixed zones in faulted poorly lithified sediments, Rio Grande rift, New Mexico, USA: Journal of Structural Geology, v. 28, p. 1623–1639, doi:10.1016/j.jsg.2006.06.008.

Rawling, G.C., Goodwin, L.B., and Wilson, J.L., 2001, Internal architecture, permeability structure, and hydrologic significance of contrasting fault zone types: Geology, v. 29, p. 43–46, doi:10.1130/0091-7613(2001)029<0043:IAPSAH>2.0.CO;2.

Russell, L.R., and Snelson, S., 1994, Structure and tectonic evolution of the Albuquerque Basin segment of the Rio Grande rift: Insights from reflection seismic data, *in* Keller, G.R., and Cather, S.M., eds., Basins of the Rio Grande Rift: Structure, Stratigraphy, and Tectonic Setting: Geological Society of America Special Paper 291, p. 83–112, doi:10.1130/SPE291-p83.

Simms, M.A., and Garven, G., 2004, Thermal convection in faulted extensional sedimentary basins: Theoretical results from finite-element modeling: Geofluids, v. 4, p. 109–130, doi:10.1111/j.1468-8115.2004.00069.x.

Taggart, J.E., and Brookins, D.G., 1975, Rb-Sr whole rock age determinations for Sandia granite and Cibola gneiss, New Mexico: Isochron/West, no. 12, p. 5–8.

Williams, A.J., Crossey, L.J., Karlstrom, K.E., Newell, D., Person, M., and Woolsey, E., 2013, Hydrogeochemistry of the Middle Rio Grande aquifer system—Fluid mixing and salinization of the Rio Grande due to fault inputs: Chemical Geology, v. 351, p. 281–298, doi:10.1016/j.chemgeo.2013.05.029.

Manuscript received 19 March 2015
Revised manuscript received 7 June 2015
Manuscript accepted 9 June 2015

Printed in USA

Geology

Tectonic controls on fault zone flow pathways in the Rio Grande rift, New Mexico, USA

Randolph T. Williams, Laurel B. Goodwin, Peter S. Mozley, Brian L. Beard and Clark M. Johnson

Geology 2015;43;723-726
doi: 10.1130/G36799.1

Notes